

## Theoretical Analysis of Radiative Effects on Transient Free Convection Heat Transfer past a Hot Vertical Surface in Porous Media

S. K. Ghosh<sup>1</sup>, O. Anwar Bég<sup>2</sup>

<sup>1</sup>Department of Mathematics, Narajole Raj College  
P.O.-Narajole, Dist.-Midnapore (West), 721 211, West Bengal, India  
g\_swapan2002@yahoo.com

<sup>2</sup>Civil Engineering Program  
R-Block, Castle College, Sheffield, S2 2RL, England, UK  
osmanbeg@sheffcol.ac.uk; docoanwarbeg@hotmail.co.uk

**Received:** 07.11.2007 **Revised:** 15.02.2008 **Published online:** 28.11.2008

**Abstract.** The purpose of the present investigation deals with the unsteady free convective flow of a viscous incompressible gray, absorbing-emitting but non-scattering, optically-thick fluid occupying a semi-infinite porous regime adjacent to an infinite moving hot vertical plate with constant velocity. We employ a Darcian viscous flow model for the porous medium. The momentum and thermal boundary layer equations are non-dimensionalized using appropriate transformations and then solved subject to physically realistic boundary conditions using the Laplace transform technique. Thermal radiation effects are simulated via a radiation-conduction parameter,  $K_r$ , based on the Rosseland diffusion approximation. The influence of Grashof (free convection) number, radiation-conduction parameter ( $K_r$ ), inverse permeability parameter ( $K_p$ ) and dimensionless time ( $t$ ) are studied graphically. We observe that increasing thermal radiation parameter causes a noticeable increase in the flow velocity,  $u$ . Temperature,  $\theta$ , is significantly increased within the boundary layer with a rise in  $K_r$  since the latter represents the relative contribution of thermal radiation heat transfer to thermal conduction heat transfer. Increased radiation therefore augments heat transfer, heats the fluid and increases the thickness of the momentum and thermal boundary layers. Velocity is found to decrease with an increase in  $K_p$  (inverse permeability parameter) as are shear stress function ( $\frac{\partial u}{\partial y}|_{y=0}$ ) magnitudes owing to greater resistance of the porous medium for lower permeabilities, which decelerate the flow. An increase in  $K_r$  however boosts the shear stress function magnitudes i.e. serves to accelerate the flow. Temperature gradient,  $\frac{\partial \theta}{\partial y}|_{y=0}$  is also positively affected by an increase in thermal radiation ( $K_r$ ) and with time. The present study has applications in geological convection, forest fire propagation, glass heat treatment processes at high temperature, metallurgical processing etc.

**Keywords:** transient, porous medium, free convection, radiation, Laplace transforms.

## 1 Introduction

Radiative-convective heat transfer flows find numerous applications in glass manufacturing, furnace technology, high temperature aerodynamics, fire dynamics and spacecraft re-entry [1]. Many studies have appeared concerning the interaction of radiative flux with thermal convection flows. For example Chang et al. [2] studied the effect of radiation heat transfer on free convection regimes in enclosures, with applications in geophysics and geothermal reservoirs. Mudan [3] studied thermal radiation heat transfer from liquid pool fires. The vast majority of convective-radiative flows have employed various algebraic approximations to the integro-differential equation of radiative heat transfer. Succinct discussions of the many models in use including the Schuster-Schwartzchild two-flux model, Milner-Eddington model, Rosseland model, P1-approximation, Chandrasekhar discrete ordinates approximation etc are provided in the monograph by Siegel and Howell [4]. In the context of spacecraft technology Sutton [5] as early as 1956 suggested that for temperatures ranging from 3500 degrees Fahrenheit to 7000 Fahrenheit, as encountered in rocket propulsion, thermal radiation can account for up to 25 % of the total heat transfer. In the internal boundary layer regimes, on rocket combustion thrust chamber walls, significant radiation heat transfer is imparted from the hot propellant to the chamber walls. Hill and Petersen [6] have highlighted the dependence of radiation heat transfer on chamber size, as the ratio of radiating volume to radiating surface is proportional to chamber size dimensions. Cheng [7] considered the radiative-convective gas dynamic flow using a differential approximation. Cess [8] presented a seminal study of radiating convective boundary layers with buoyancy effects using the Rosseland diffusion approximation. Further studies in the context of boundary layer aerodynamics were communicated by Tabaczynski and Kennedy [9], Taitel and Hartnett [10], Cogley et al. [11] who considered non-grey gases, England and Emery [12] who analyzed absorption effects of the gas, Adunson and Gebhart [13], Bankston et al. [14] who considered both absorption and emission properties of the fluid and Dombrowski [15] who reported on optically-thick flat plate boundary layers. Yucel and Bayazitoglu [16] analyzed the more complex case of anisotropical scattering in boundary layer radiative-convection. Hossain and Takhar [17] studied the mixed convection flat plate boundary layer problem using the Rosseland (diffusion) flux model. The above studies did not consider transient effects or incorporate porous media effects. Both unsteady flows and porous convective-radiative flows have important applications in geophysics, geothermics, chemical and ceramics processing. The conventional approach in porous media transport modeling has been to simulate the pressure drop across the porous regime using the Darcy linear model. This basically adds an extra body force to the momentum boundary layer equation. Bear [18] has provided an excellent treatment of Darcian hydromechanics, which is valid for viscous-dominated flows generally to a Reynolds number of about 10. Kaviany [19] has provided an excellent appraisal of Darcian thermal convection flows and also coupled convective-radiative heat transfer in porous media. Several studies have appeared recently analyzing the effects of thermal radiation in convection flows in porous media. Takhar et al. [20] studied the dissipative radiative-convection of a gas in a porous medium using the differential approximation, with applications in geothermal energy systems. Chamkha [21] studied the

solar radiation effects on porous media convection on a vertical surface with applications in solar collector dynamics. Mohammadein et al. [22] studied the radiative flux effects on free convection in Darcian porous media with the Rosseland model. Satapathy et al. [23] and El-Hakiem et al. [24] have also analyzed radiative-convection flows in non-Darcian porous media using asymptotic and numerical methods. The 2-flux Schuster-Schwartzchild model was used by Nagaraju et al. [25] to study convective-radiative flows in variable permeability regimes using the Blottner difference scheme. Takhar et al. [26] used shooting quadrature to analyze the mixed convection flow with thermal radiation effects in Darcy-Forchheimer porous media. More recently Chamkha et al. [27] studied Rosseland radiation-conduction number effects on boundary layer wedge convection of a viscoelastic fluid in non-Darcian porous material. All of the above studies however were for steady flows. The effect of unsteadiness in porous media and purely fluid regime convection is important in numerous energy and environmental systems. Several authors have therefore studied transient radiative-convective heat (and mass) transfer flows in pure fluids or porous media. Ganesan et al. [28] studied theoretically the thermal radiation effects on unsteady flow past an impulsively started plate. Muthucumaraswamy and Ganesan [29] analyzed transient radiation-convection impulsively-started flow with variable temperature effects. Ghosh and Pop [30] studied indirect radiation effects on convective gas flow. Raptis and Perdakis [31] have also studied analytically the transient convection in a highly porous medium with unidirectional radiative flux. Very recently Zueco et al. [31] have presented two-dimensional numerical solutions for non-Darcian radiation-convection heat and mass transfer from an impulsively-started vertical surface in porous media. In the present study we consider analytically the transient convective-radiative heat transfer in an isotropic, homogenous porous regime adjacent to a hot vertical plate using the Laplace transform method. Such a study has not appeared in the literature and constitutes an important addition to the area of porous media convection studies.

## 2 Mathematical model

We consider the unsteady flow of a viscous incompressible fluid occupying a semi-infinite region of the space past an infinite hot vertical plate moving upwards with constant velocity embedded in a porous medium, as depicted in Fig. 1. The co-ordinate system is selected such that the  $x'$ -axis is directed along the plate from the leading edge in the vertically upward direction and the  $y'$ -axis is normal to the plate. All fluid properties are considered constant except the influence of density variation in the body force term, under the Oberbeck-Boussinesq approximation. The radiation heat flux in the  $x'$ -direction is considered negligible in comparison to the  $y'$ -direction. The fluid is gray, absorbing-emitting but non-scattering. Gravity acts in the opposite direction to the positive  $x'$ -axis. The porous regime is assumed to be in local thermal equilibrium and thermal dispersion effects are ignored. The unsteady boundary layer equations for mass, momentum and energy (heat) conservation under these approximations, neglecting convective inertial

terms, can be shown to take the form:

$$\frac{\partial u'}{\partial x'} + \frac{\partial v'}{\partial y'} = 0, \tag{1}$$

$$\frac{\partial u'}{\partial t'} = \nu \frac{\partial^2 u'}{\partial y'^2} + g\beta(T' - T'_\infty) - \frac{\nu u'}{K}, \tag{2}$$

$$\frac{\partial T'}{\partial t'} = \frac{k_1}{\rho C_p} \frac{\partial^2 T'}{\partial y'^2} - \frac{1}{\rho C_p} \frac{\partial q_r}{\partial y'}. \tag{3}$$

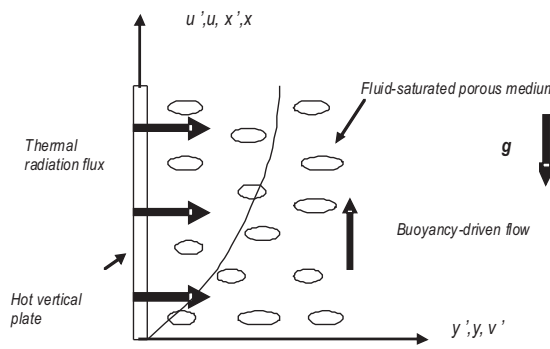


Fig. 1. Physical model and co-ordinate system.

The appropriate boundary conditions at the wall and in the free stream are:

$$\begin{aligned} u' = 0, \quad T' = T'_\infty \quad \text{for } y' \geq 0, \quad t' \leq 0, \\ u' = U, \quad T' = T'_w \quad \text{for } y' = 0, \quad t' > 0, \\ u' = 0, \quad T' \rightarrow T'_\infty \quad \text{for } y' \rightarrow \infty, \end{aligned} \tag{4}$$

where  $u', v', t', \nu, g, \beta, T', T'_\infty, k_1, C_p, \rho, q_r$  and  $K$  are, respectively, the velocity component along the plate, the velocity component normal to the plate, dimensional time, the kinematic coefficient of viscosity, the gravitational acceleration, the coefficient of thermal expansion, the temperature of the fluid, the temperature of the fluid far away from the plate (in the free stream), the thermal conductivity, the specific heat at constant pressure, the density of the fluid, the radiative heat flux and the permeability of the porous medium (dimensions,  $m^2$ ). Also  $T'_w$  is the temperature at the plate and  $U$  is the velocity of the moving plate. The radiation flux on the basis of the Rosseland diffusion model for radiation heat transfer is expressed as:

$$q_r = -\frac{4\sigma^*}{3k^*} \frac{\partial T'^4}{\partial y'}, \tag{5}$$

in which  $\sigma^*$  and  $k^*$  are Stefan-Boltzmann constant and the spectral mean absorption coefficient of the medium. It is assumed that the temperature differences within the flow

are sufficiently small such that  $T'^4$  may be expressed as linear function of the temperature. It can be established by expanding  $T'^4$  in a Taylor series about  $T'_\infty$  and neglecting higher order term, that  $T'^4$  can be expressed in the following way:

$$T'^4 = 4T'^3_\infty T' - 3T'^4_\infty. \quad (6)$$

Implementing equations (5) and (6) in equation (3) we arrive at the modified energy conservation equation:

$$\frac{\partial T'}{\partial t'} = \frac{k_1}{\rho C_p} \frac{\partial^2 T'}{\partial y'^2} + \frac{1}{\rho C_p} \frac{4\sigma^*}{3k^*} \frac{\partial^2 T'^4}{\partial y'^2}. \quad (7)$$

To present solutions which are independent of the geometry of the flow regime, we introduce a series of non-dimensional transformations, defined as:

$$\begin{aligned} u &= \frac{u'}{U} && \text{(dimensionless velocity),} \\ y &= \frac{y'U}{\nu} && \text{(non-dimensional distance),} \\ t &= \frac{t'U^2}{\nu} && \text{(dimensionless time),} \\ \theta &= \frac{T' - T'_\infty}{T'_w - T'_\infty} && \text{(dimensionless temperature),} \\ Pr &= \frac{\rho\nu C_p}{k_1} && \text{(Prandtl number),} \\ Gr &= \frac{g\beta\nu(T'_w - T'_\infty)}{U^3} && \text{(Grashof number),} \\ Kr &= \frac{16\sigma^*T'^3_\infty}{3k^*k_1} && \text{(radiation-conduction parameter),} \\ K_p^2 &= \frac{\nu^2}{KU^2} && \text{(inverse permeability parameter for the porous medium).} \end{aligned} \quad (8)$$

The continuity equation is satisfied and equations (2) and (7) are thereby transformed to:

$$\frac{\partial u}{\partial t} = \frac{\partial^2 u}{\partial y^2} + Gr\theta - K_p^2 u, \quad (9)$$

$$(1 + Kr) \frac{\partial^2 \theta}{\partial y^2} - Pr \frac{\partial \theta}{\partial t} = 0. \quad (10)$$

The corresponding boundary conditions are

$$\begin{aligned} u = 0, \quad \theta = 0 & \quad \text{for } y \geq 0, \quad t \leq 0, \\ u = 1, \quad \theta = 1 & \quad \text{for } y = 0, \quad t > 0, \\ u = 0, \quad \theta \rightarrow 0 & \quad \text{for } y \rightarrow \infty, \end{aligned} \quad (11)$$

### 3 Analytical solution

By employing the Laplace transform technique the solutions to the linear partial differential equations (9) and (10) for the transient velocity ( $u$ ) and transient temperature ( $\theta$ ) subject to the boundary conditions (11) can be shown to take the following form:

$$\begin{aligned}
 u(y, t) = & \frac{1}{2} \left( 1 - \frac{Gr}{K_p^2} \right) \\
 & \times \left[ \exp(-K_p y) \operatorname{erfc} \left( \frac{y - 2K_p t}{2\sqrt{t}} \right) + \exp(K_p y) \operatorname{erfc} \left( \frac{y + 2K_p t}{2\sqrt{t}} \right) \right] \\
 & + \frac{Gr}{K_p^2} \operatorname{erfc} \left( \frac{y}{2} \sqrt{\frac{Pr}{(1 + K_r)t}} \right) \\
 & + \frac{Gr}{K_p^2} \frac{y}{2\sqrt{\pi}} \frac{(\sqrt{2} - 1)t^{-1/2}}{2} \\
 & \times \left[ \exp \left\{ - \left( \frac{y^2}{4t} + K_p^2 t \right) \right\} - \sqrt{\frac{Pr}{1 + K_r}} \exp \left( - \frac{y^2}{4t} \frac{Pr}{1 + K_r} \right) \right], \quad (12)
 \end{aligned}$$

$$\theta(y, t) = \operatorname{erfc} \left( \frac{y}{2} \sqrt{\frac{Pr}{(1 + K_r)t}} \right). \quad (13)$$

In these solutions we can extract the cases for the purely fluid regime i.e. infinite permeability by setting  $K_p \rightarrow 0$ . For the cases where thermal radiation is absent we set  $K_r \rightarrow 0$ . Dimensionless shear stress at the wall is evaluated by differentiating the velocity  $u$  with respect to  $y$ . Dimensionless heat transfer at the wall is computed by obtaining the gradient of the temperature solution with respect to  $y$ . The expressions for shear stress function i.e. velocity gradient,  $\frac{\partial u}{\partial y}|_{y=0}$  and surface heat transfer rate i.e. temperature gradient,  $\frac{\partial \theta}{\partial y}|_{y=0}$  take the form:

$$\begin{aligned}
 \frac{\partial u}{\partial y} \Big|_{y=0} = & \frac{1}{2} \left( 1 - \frac{Gr}{K_p^2} \right) \\
 & \times \left[ (-K_p) \operatorname{erfc}(-K_p \sqrt{t}) (K_p) \operatorname{erfc}(K_p \sqrt{t}) - \frac{2}{\sqrt{t\pi}} \exp(-K_p^2 t) \right] \\
 & - \frac{Gr}{K_p^2} \frac{1}{\sqrt{\pi}} \left[ \sqrt{\frac{Pr}{(1 + K_r)t}} \right] \\
 & + \frac{Gr}{K_p^2} \frac{1}{4\sqrt{\pi}} (\sqrt{2} - 1)t^{-1/2} \left[ \exp \left\{ -K_p^2 t \right\} - \sqrt{\frac{Pr}{1 + K_r}} \right], \quad (14)
 \end{aligned}$$

$$\frac{\partial \theta}{\partial y} \Big|_{y=0} = -\frac{1}{\sqrt{\pi}} \left( \sqrt{\frac{Pr}{(1 + K_r)t}} \right). \quad (15)$$

#### 4 Results and discussion

To gain a perspective of the physics of the flow regime, we have numerically evaluated the effects of Grashof number ( $Gr$ ), radiation-conduction parameter ( $K_r$ ), dimensionless time ( $t$ ) and inverse permeability parameter ( $K_p$ ), on the velocity,  $u$ , temperature,  $\theta$ , shear stress function (velocity gradient i.e.  $\frac{\partial u}{\partial y}|_{y=0}$ ) and surface heat transfer function (temperature gradient i.e.  $\frac{\partial \theta}{\partial y}|_{y=0}$ ). Figs. 2 to 10 present these computations graphically. As default values we set  $K_p = 1$ ,  $K_r = 1$  (which implies equal radiation and conduction contribution),  $Gr = 2$  (buoyancy force is twice the viscous hydrodynamic force in the boundary layer),  $Pr = 0.72$  (which corresponds to air),  $t = 0.2$ . These values apply unless otherwise indicated.

In Fig. 2, the spatial distribution of velocity,  $u$ , is plotted for the effects of inverse permeability parameter ( $K_p$ ), at a fixed time,  $t = 0.2$ . As the inverse permeability parameter,  $K_p$ , increases from 1 to 2 and then 3, the velocity,  $u$ , continuously decreases with distance transverse to the wall. The parameter  $K_p$  as defined in equation (8) is *inversely* proportional to the *actual permeability*,  $K$ , of the porous medium. The Darcian drag force in the momentum equation, viz,  $-K_p^2 u$ , is therefore directly proportional to  $K_p$ . An increase in  $K_p$  will therefore increase the resistance of the porous medium (as the permeability physically becomes less with increasing  $K$ ) which will serve to decelerate the flow and reduce velocity,  $u$ . This trend is indeed maintained with further separation from the plate. At  $y = 2$  we observe that the streamwise velocity ( $u$ ) decreases from 0.065299 for  $K_p = 1$  to very close to zero for  $K_p = 2$ , and is further reduced to the minimum for  $K_p = 3$ . Deceleration of the flow is therefore sustained at considerable distance from the plate towards the free stream as inverse permeability ( $K_p$ ) parameter is increased. The profiles decay monotonically for all values of  $K_p$  from the maximum at the wall to the minimum in the free stream.

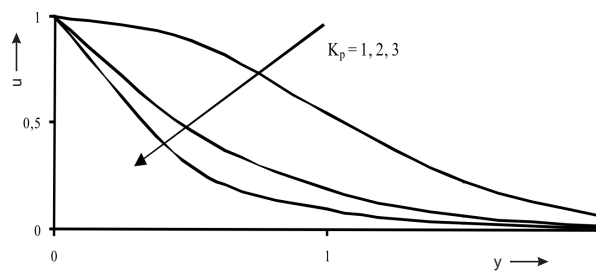


Fig. 2. Non-dimensional spatial velocity distribution ( $u$ ) for  $Gr = 2.0$ ,  $K_r = 1.0$ ,  $Pr = 0.72$  and  $t = 0.2$  for various inverse permeability parameters ( $K_p$ ).

In Fig. 3 we have plotted the spatial variation of dimensionless velocity ( $u$ ) with radiation-conduction parameter,  $K_r$ , again at  $t = 0.2$ , for weak free convection ( $Gr = 2$ ) and high permeability ( $K_p = 1$ ). The parameter,  $K_r$ , defines the relative contribution of radiation heat transfer to thermal conduction transfer. Large  $K_r$  values imply large

radiation contribution, as may be encountered in for example high temperature materials processing applications, glass production etc. In the limit as  $K_r \rightarrow 0$ , thermal radiation flux contribution vanishes i.e. the regime is *free* convection with thermal conduction at the wall. In the opposite limit as  $K_r \rightarrow \infty$ , thermal radiation totally dominates thermal conduction. Hence with an increase in  $K_r$ , *thermal radiation* will have a stronger contribution than *thermal conduction* (the contribution is only equal for both modes of heat transfer when  $K_r = 1$ ). Velocity,  $u$  is seen therefore to increase in magnitude with a rise in  $K_r$  i.e. increase in thermal radiation contribution. An interesting feature for the highest  $K_r$  value is the presence of an overshoot in velocity over the range  $0 < y < 0.7$ . Velocity rises above the prescribed value at the wall (unity) peaks at  $y \sim 0.5$ , and then falls progressively thereafter. This trend is not observed for  $K_r = 1$  or 2. Thermal radiation supplements the fluid thermal conductivity via the energy equation and serves to increase buoyancy and therefore accelerates the flow. We observe in consistency with this that for example for  $y = 1.0$ ,  $u$  increases in value from  $K_r = 0.5$  (thermal conduction is greater than radiation for  $K_r < 1$ ), to  $K_r = 1$  and then to the maximum value at this location, for  $K_r = 2.0$ . Similarly this pattern of increase in velocity is sustained with greater distance from the wall. At  $y = 2$  (maximum computed distance from the plate), dimensionless velocities are all minimized although again the values are highest for the highest value of  $K_r$ .

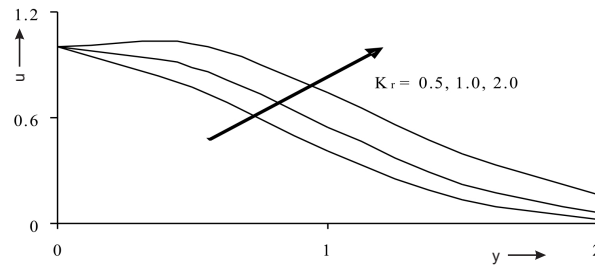


Fig. 3. Non-dimensional spatial velocity distribution ( $u$ ) for  $Gr = 2.0$ ,  $K_p = 1.0$ ,  $Pr = 0.72$  and  $t = 0.2$  for various inverse permeability parameters ( $K_r$ ).

The profiles of spatial dimensionless velocity ( $u$ ) with distance from the wall, at various times ( $t$ ) are shown in Fig. 4. As time,  $t$ , increases from 0.2, 0.3 to 0.4 we observe that velocity  $u$  is increased markedly. There is a steep decline from the wall for all profiles and no velocity overshoot. With time the flow is therefore accelerated in the upward direction. Values of  $u$  at any distance  $y$  are always higher for  $t = 0.4$  than for  $t = 0.3$  or  $t = 0.2$ . Peak velocity always occurs at the wall owing to the translational of the wall in the upward direction, according to the dimensionless boundary condition imposed.

In Fig. 5 we have studied the influence of buoyancy via the Grashof number ( $Gr$ ), on the velocity development with distance normal to the wall at time,  $t = 0.2$ . We observe that consistently the velocity,  $u$ , is increased with distance,  $y$ , as  $Gr$  is increased from



2 to 4 and then 6. The flow is accelerated due to the enhancement in buoyancy forces corresponding to an increase in Grashof number i.e. free convection effects. Positive values of  $Gr$  correspond to cooling of the plate surface by natural convection. Heat is therefore conducted away from the vertical plate into the fluid which increases temperature and thereby enhances the buoyancy force. For the higher values of  $Gr$  (i.e. 4, 6) there are velocity overshoots close to the moving plate (at  $y \sim 0.5$ ) after which profiles descend smoothly to their lowest values, in the free stream. For  $Gr = 2$  no such overshoot is observed. As such only much larger buoyancy forces (i.e.  $Gr = 4, 6$ ) would be responsible for the overshoot effect. As before with the effects of thermal radiation parameter ( $K_r$ ) the increase in velocity is sustained at further distances from the wall i.e.  $u$  values are highest for  $Gr = 6.0$  (maximum thermal Grashof number) for all values of  $y$ , except at the wall where velocity is held at unity.

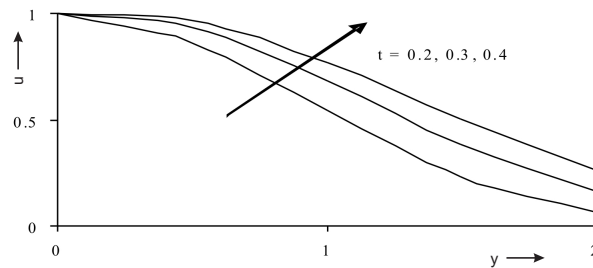


Fig. 4. Non-dimensional spatial velocity distribution ( $u$ ) for  $Gr = 2.0$ ,  $K_r = 1.0$ ,  $K_p = 1.0$ ,  $Pr = 0.72$  for various times ( $t$ ).

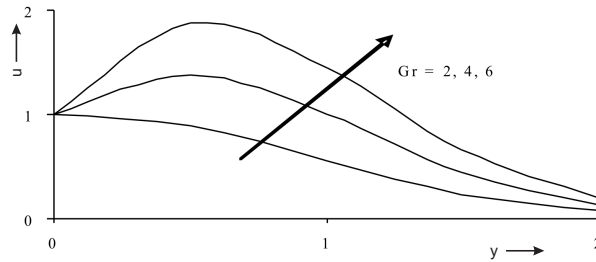


Fig. 5. Non-dimensional spatial velocity distribution ( $u$ ) for  $K_r = 1.0$ ,  $K_p = 1.0$ ,  $Pr = 0.72$ ,  $t = 0.2$  for various Grashof numbers ( $Gr$ ).

The effects of time ( $t$ ) and radiation-conduction parameter ( $K_r$ ) on spatial distribution of the dimensionless temperature function ( $\theta$ ) are shown in Figs. 6 and 7. Temperature in Fig. 6 is seen to decrease from a maximum at the wall (1.0) to a minimum value with maximum distance,  $y$ . However with increasing time ( $t$ ) we observe that there is a clear increase in temperatures. This trend is maintained at all locations in the flow regime

i.e. velocity at  $y = 1.0, 1.5$  or  $2.0$  is always maximized with the greatest time ( $t = 0.4$ ). Fig. 7 shows that at fixed time,  $t = 0.2$ , an increase in thermal radiation-conduction parameter ( $K_r$ ) is observed to strongly increase temperatures throughout the fluid with distance normal to the wall in the porous medium regime. Larger  $K_r$  values correspond to an increased dominance of thermal radiation over conduction. As such thermal radiation supplements the thermal diffusion and increases the overall thermal diffusivity of the regime since the Rosseland diffusion flux model adds a radiation conductivity to the conventional thermal conductivity. As a result the temperatures in the porous medium flow (which has high permeability as  $K_p$  is fixed in Fig. 7) are significantly increased. Since the medium is highly absorbing, thermal boundary layer thicknesses will also be increased.

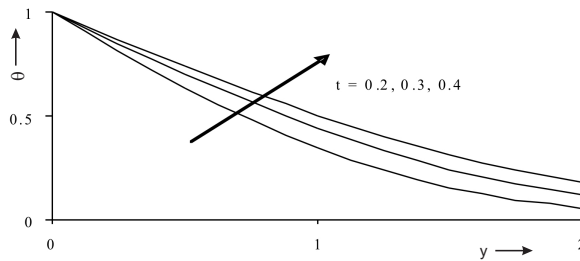


Fig. 6. Dimensionless temperature profile ( $\theta$ ) for  $K_r = 1.0, K_p = 1, Gr = 2.0, Pr = 0.72$  for various dimensionless times ( $t$ ).

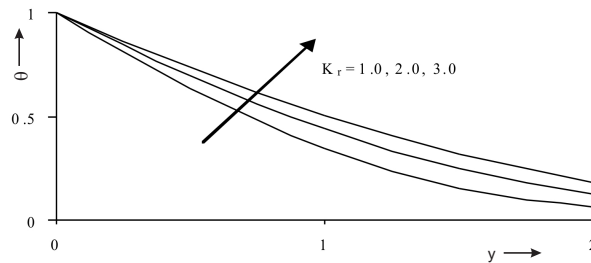


Fig. 7. Dimensionless temperature profile ( $\theta$ ) for  $Pr = 0.72, K_p = 1, Gr = 2.0$  for various radiation-conduction parameters ( $K_r$ ).

In Fig. 8 the variation of the velocity gradient (i.e. shear stress function),  $\frac{\partial u}{\partial y}|_{y=0}$  with inverse permeability parameter ( $K_p$ ) and also thermal radiation-conduction parameter ( $K_r$ ). As expected with an increase in  $K_p$  (corresponding to a decrease in permeability) the magnitude of shear stress function is decreased considerably, as shown by the negative slope of the profiles. Conversely with a rise in  $K_r$ , shear stress function is positively affected indicating that the presence of thermal radiation accelerates the flow, an important feature in metallurgical materials processing.

In Fig. 9 the collective influence of the Grashof number ( $Gr$ ) and thermal radiation-conduction parameter ( $K_r$ ) on the shear stress function variation is shown. Increasing  $Gr$  clearly increases shear stress function ( $\frac{\partial u}{\partial y}|_{y=0}$ ) values i.e. increasing buoyancy serves to accelerate the flow which increases shear stress function values. Similarly in consistency with previous computations, an increase in thermal radiation also serves to accelerate the flow which increases shear stress function values i.e. the maximum shear stress function,  $\frac{\partial u}{\partial y}|_{y=0}$ , corresponds to the maximum  $K_r$  value (highest thermal radiation flux).

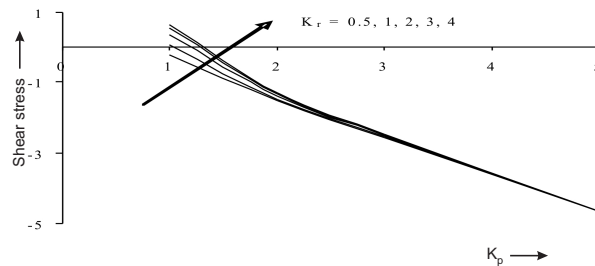


Fig. 8. Shear stress function at the plate for  $Pr = 0.72$ ,  $Gr = 2.0$  and  $t = 0.2$  for various radiation-conduction parameters ( $K_r$ ) and inverse permeability parameter ( $K_p$ ).

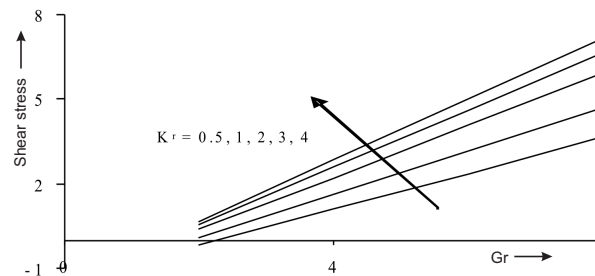


Fig. 9. Shear stress function at the plate for  $Pr = 0.72$ ,  $t = 0.2$  and  $K_p = 1.0$  and various Grashof numbers ( $Gr$ ) and radiation-conduction parameters ( $K_r$ ).

Finally in Fig. 10, we observe that with an increase in thermal radiation-conduction parameter,  $K_r$  (i.e. the abscissa coordinate) the temperature gradient at the wall is increased i.e. values become less negative with increasing  $K_r$ . Similarly with increasing time from 0.2 through 0.3, 0.4, 0.5 to 0.6, there is a consistent increase in temperature gradient,  $\frac{\partial \theta}{\partial y}|_{y=0}$ . Both thermal radiation flux and time therefore have a positive influence on heat transfer from the plate surface into the porous medium.

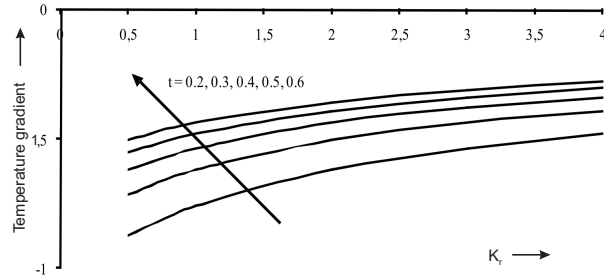


Fig. 10. Temperature gradient ( $\frac{\partial \theta}{\partial y}|_{y=0}$ ) at the wall for  $Pr = 0.72$  and  $K_p = 1.0$  for various radiation-conduction parameters ( $K_r$ ) and times ( $t$ ).

## 5 Conclusions

A mathematical model has been presented for the unsteady convection heat transfer from a vertical translating plate adjacent to a Darcian porous medium, in the presence of significant thermal radiation. The governing boundary layer equations have been non-dimensionalized and solved using the Laplace transform technique. It has been shown that the fluid is accelerated i.e. velocity ( $u$ ) is increased with a rise in permeability of the porous medium (i.e. a decrease in inverse permeability parameter ( $K_p$ )), with increasing thermal radiation-conduction parameter ( $K_r$ ), time ( $t$ ) and also free convection parameter (Grashof number,  $Gr$ ). Dimensionless temperature ( $\theta$ ) is also seen to increase with time ( $t$ ) and increasing  $K_r$  values, owing to an increase in radiation which augments buoyancy in the porous regime. An increase in inverse permeability parameter (corresponding to lesser permeability of the porous regime) also reduces the shear stress function ( $\frac{\partial u}{\partial y}|_{y=0}$ ) values. Conversely increasing Grashof number and thermal radiation-conduction parameter serve to increase shear stress function values. Temperature gradient,  $\frac{\partial \theta}{\partial y}|_{y=0}$ , is increased by a rise in thermal radiation-conduction parameter and also with time.

## Acknowledgements

The authors wish to thank both reviewers for their excellent comments which have helped significantly to improve the quality of this paper. We are also grateful to Dr S. Rawat of the Mathematics Department, Indian Institute of Technology, for his gracious assistance in the preparation of the figures.

## References

1. H. C. Hottel, A. Sarofim, *Radiation Heat Transfer*, MacGraw Hill, 1967.
2. L. C. Chang, K. T. Yang, J. R. Lloyd, Radiation-natural convection interactions in two-dimensional complex enclosures, *ASME J. Heat Transfer*, **105**, pp. 89–95, 1983.

3. K. S. Mudan, Thermal radiation hazards from hydrocarbon pool fires, *Prog. Energy Combustion Science*, **10**, pp. 59–80, 1984.
4. R. Siegel, J. R. Howell, *Thermal Radiation Heat Transfer*, Hemisphere, USA, 1993.
5. G. P. Sutton, *Rocket Propulsion Elements*, New York, John Wiley & Sons, 1956.
6. P. G. Hill, C. R. Peterson, *Mechanics and Thermodynamics of Propulsion*, 2nd edition, Addison-Wesley, Reading, Massachusetts, USA, 1967.
7. P. Cheng, *Study of the Flow of a Radiating Gas by a Differential Approximation*, PhD, Stanford University, California, 1965.
8. R. D. Cess, The interaction of thermal radiation with free convection heat transfer, *Int. J. Heat Mass Transfer*, **9**, pp. 1269–1277, 1966.
9. R. J. Tabaczynski, L. A. Kennedy, Thermal radiation effects in laminar boundary layer flow, *AIAA Journal*, **5**, pp. 1893–1894, 1967.
10. Y. Taitel, J. P. Hartnett, Equilibrium temperatures in boundary layer flow over a flat plate of absorbing-emitting gas, *ASME J. Heat Transfer*, **90**, pp. 257–266, 1968.
11. A. C. Cogley, W. G. Vincenti, S. E. Giles, Differential approximation for radiative transfer in a non-grey gas near equilibrium, *AIAA J.*, pp. 551–553, 1968.
12. W. G. England, A. F. Emery, Thermal radiation effects on the laminar free convection boundary layer of an absorbing gas, *ASME J. Heat Transfer*, **91**, 37–48, 1969.
13. T. Adunson, B. Gebhart, An experimental and analytical study of natural convection with appreciable thermal radiation effects, *J. Fluid Mechanics*, **52**, pp. 57–95, 1972.
14. J. D. Bankston, J. R. Lloyd, J. L. Novotny, Radiation-convection interaction in an absorbing-emitting liquid in natural convection boundary layer flow, *ASME J. Heat Transfer*, **99**, pp. 125–127, 1977.
15. L. A. Dombrowski, Radiation-convection heat transfer by an optically-thick boundary layer on a plate, *High Temperature*, **19**, pp. 100–109, 1981.
16. A. Yucel, Y. I. Bayazitoglu, Radiative heat transfer in absorbing, emitting and anisotropically scattering boundary layer, AIAA paper No. 83-1504, American Institute of Aeronautics and Astronautics, 1983.
17. M. A. Hossain, H. S. Takhar, Radiation effects on mixed convection along a vertical plate with uniform surface temperature, *Heat and Mass Transfer*, **31**, pp. 243–248, 1996.
18. J. Bear, *Dynamics of Fluids in Porous Media*, Dover, New York, 1988.
19. M. Kaviany, *Principles of Heat Transfer in Porous Media*, MacGraw-Hill, New York, 1993.
20. H. S. Takhar, O. A. Bég, M. Kumari, Computational analysis of coupled radiation-convection dissipative non-gray gas flow in a non-Darcy porous medium using the Keller-Box implicit difference scheme, *Int. J. Energy Research*, **22**, pp. 141–159, 1998.
21. A. J. Chamkha, Solar radiation assisted natural convection in a uniform porous medium supported by a vertical flat plate, *ASME J. Heat Transfer*, **119**, pp. 89–96, 1997.

22. A. A. Mohammadein, M. A. Mansour, S. M. El Gaied, R. S. R. Gorla, Radiative effect on natural convection flows in porous media, *Transport Porous Media*, **32**(3), pp. 263–283, 1998.
23. S. Satapathy, A. Bedford, S. Bless, A. Raptis, Radiation and free convection flow through a porous medium, *Int. Comm. Heat Mass Transfer*, **25**(2), pp. 289–297, 1998.
24. M. A. El-Hakiem, R. S. R. Gorla, Radiative effects in non-Darcy axisymmetric free convection in a porous medium, *Int. J. Applied Mechanics Engineering*, **5**(4), pp. 913–921, 2000.
25. P. Nagaraju, A. J. Chamkha, H. S. Takhar, B. C. Chandrasekhara, Simultaneous radiative and convective heat transfer in a variable porosity medium, *Heat and Mass Transfer J.*, **37**, pp. 243–250, 2001.
26. H. S. Takhar, O. A. Bég, A. J. Chamkha, D. Filip, I. Pop, Mixed radiation-convection boundary layer flow of an optically dense fluid along a vertical flat plate in a non-Darcy porous medium, *Int. J. Applied Mechanics Engineering*, **8**, pp. 483–496, 2003.
27. A. J. Chamkha, H. S. Takhar, O. A. Bég, Radiative free convective non-Newtonian fluid flow past a wedge embedded in a porous medium, *Int. J. Fluid Mechanics Research*, **31**, pp. 101–115, 2004.
28. P. Ganesan, P. Loganathan, V. M. Soundalgekar, Radiation effects on flow past an impulsively started plate, *Int. J. Applied Mechanics Engineering*, **6**(3), pp. 719–730, 2001.
29. R. Muthucumaraswamy, P. Ganesan, Radiation effects on flow past an impulsively started infinite vertical plate with variable temperature, *Int. J. Applied Mechanics Engineering*, **8**(1), pp. 125–129, 2003.
30. S. K. Ghosh, I. Pop, Thermal radiation of an optically thin gray gas in the presence of indirect natural convection, *Int. J. Fluid Mechanics Research*, **34**(6), pp. 515–520, 2007.
31. A. Raptis, C. Perdakis, Unsteady flow through a highly porous medium in the presence of radiation, *Transport Porous Media J.*, **57**(2), pp. 171–179, 2004.
32. J. Zueco, H. S. Takhar, R. S. R. Gorla, O. A. Bég, Network simulation of thermal radiation, non-Darcy and impulsive effects on unsteady two-dimensional natural convective heat and mass transfer in porous media, 2007 (submitted).